Frequency-Domain Oversampling for Zero-Padded OFDM in Underwater Acoustic Communications

Zhaohui Wang[1], Shengli Zhou[1], Georgios B. Giannakis[2], Christian R. Berger[3], and Jie Huang[1]

[1]Department of Electrical and Computer Engineering, University of Connecticut, Storrs, CT 06250
[2]Department of Electrical and Computer Engineering, University of Minnesota, Minneapolis, MN 55455
[3]Department of Electrical and Computer Engineering, Carnegie Mellon University, Pittsburgh, PA 15213

***Abstract*— Although time-domain oversampling of the received baseband signal is common for single-carrier transmissions, the counterpart of frequency-domain oversampling is rarely used for multicarrier transmissions. In this paper, we explore frequency-domain oversampling to improve the system performance of zero-padded OFDM transmissions over underwater acoustic channels with large Doppler spread. We use a signal design that enables separate sparse channel estimation and data detection, rendering a low complexity receiver. Based on both simulation and experimental results, we observe that the receiver with frequency-domain oversampling outperforms the conventional one considerably in channels with moderate and large Doppler spreads, and the gain increases as the Doppler spread increases. Although a raised-cosine pulse-shaping window can be used to improve the system performance relative to a rectangular window at the expense of data rate reduction, the performance gain is much less than that brought by frequency-domain oversampling in the considered OFDM system for Doppler spread channels.**

***Index Terms*— OFDM, zero-padding, inter-carrier interference, Doppler spread, frequency-domain oversampling.**

I. Introduction

Recently, zero-padded (ZP) orthogonal frequency division multiplexing (OFDM) has been extensively investigated for high data rate underwater acoustic communications [1]–[3]. Following Doppler shift compensation and an overlap-adding operation, fast-Fourier transform (FFT) is performed on the received block to obtain frequency-domain samples, that are used for subsequent channel estimation and data detection [1]–[3]. However, overlap-adding operation incurs information loss: it folds a received block that is a linear convolution of the input and the channel, into a *shorter* block that corresponds to a circular convolution of the input and the channel. This fact has been recognized in [4], and other forms of receivers have been developed to improve the system performance.

In this paper, we investigate the use of frequency-domain oversampling for ZP-OFDM to improve the system performance over underwater acoustic channels with large Doppler spread. At the outset, this paper distinguishes itself from [4] in the following aspects: (i) The receivers in [4] are based on a time-invariant channel, while this paper considers time-varying channels with large Doppler spread; (ii) The receivers in [4] assume perfect channel knowledge, while this paper deals with both channel estimation and data detection; (iii) The performance results in [4] are based on simulations only, where the block sizes are much smaller than typical values used in practical systems. This paper validates the system performance using real data collected from field experiments.

This work is supported by the ONR grants N00014-07-1-0805 (YIP), N00014-09-1-0704 (PECASE), and the NSF grant CNS-0721834.

We use the OFDM signals in [5] designed for underwater channels with large Doppler spread. In addition to the rectangular pulse-shaping window, we also include raised-cosine windows in our transmitter design. We develop a receiver with frequency-domain oversampling, using compressive sensing techniques for sparse channel estimation and MMSE equalization for data detection. We evaluate the performance of the proposed receiver using both simulation and real data collected from the SPACE08 experiment , held off the coast of Martha's Vineyard, Massachusetts, 2008, and the WHOI09 experiment, held in the Buzzards Bay, Massachusetts, 2009. Simulation results show that frequency-domain oversampling improves the system performance considerably, and the performance gain increases as the channel Doppler spread increases. Experimental results verify the benefits of frequency-domain oversampling, achieving similar performance with fewer phones than the receiver without oversampling. Interestingly, although a raised-cosine pulse-shaping window can improve the system performance relative to a rectangular window, the performance gain is much less than that brought by frequency-domain oversampling in the considered OFDM system, despite the fact that a raised-cosine pulse-shaping incurs a data rate reduction.

Note that the time-domain oversampling is commonly used for single-carrier transmissions [6]. Its dual, the frequency-domain oversampling, is rarely used for multicarrrier transmissions. So far, we are only aware of [7], where it is used for blind carrier-frequency-offset recovery, and [8], where it is used to exploit the multipath diversity of time-invariant and narrowband channels in wireless communications.

The rest of the paper is as follows. The system model is introduced in Section II. The proposed transmitter and receiver designs are presented in Section III. Numerical simulations are given in Section IV and experimental results are collected in Sections V and VI. We conclude in Section VII.

Notation: Bold upper-case and lower-case letters denote matrices and column vectors, respectively; $(\cdot)^T$, $(\cdot)^*$, and $(\cdot)^H$ denote transpose, conjugate, and Hermitian transpose, respectively. $\mathbf{I}_N$ stands for an identity matrix with size N.

II. System Model And Motivation

Zero-padded OFDM with a rectangular pulse-shaping window has been used in [1]–[3]. In this paper, we extend the

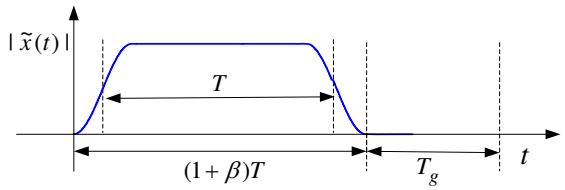

(a) One transmitted ZP-OFDM block

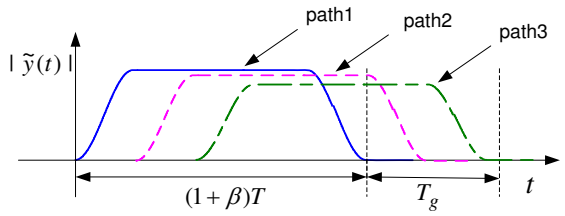

(b) One received ZP-OFDM block

Fig. 1. Illustration of the transmitted and received signals in the time domain.

system formulation to include a raised-cosine pulse-shaping window. With T denoting the symbol duration, and β denoting the roll-off factor, the raised-cosine window is [6]

$$g(t) = \begin{cases} 1, & t \in \left[\frac{\beta}{2}T, T\right] \\ \frac{1}{2}\left[1+\cos\left(\frac{\pi}{\beta T}\left(\left|t-\frac{1+\beta}{2}T\right|-\frac{1-\beta}{2}T\right)\right)\right], & t \in \left[0, \frac{\beta}{2}T\right) \cup (T, (1+\beta)T] \\ 0, & \text{otherwise} \end{cases} \quad (1)$$

whose Fourier transform is

$$G(f) = \frac{\sin(\pi f T)}{\pi f T} \cdot \frac{\cos(\pi\beta f T)}{1-4\beta^2 f^2 T^2} e^{-j\pi f(1+\beta)T}. \quad (2)$$

When $\beta = 0$, $g(t)$ in (1) reduces to the rectangular window.

With the symbol duration of T, the subcarrier spacing is $1/T$, and the subcarriers are located at the frequencies

$$f_k = f_c + k/T, \qquad k = -K/2, \ldots, K/2-1, \quad (3)$$

where f_c is the center frequency and K is the total number of subcarriers. Define $\mathcal{S}_A$ and $\mathcal{S}_N$ as the non-overlapping sets of active and null subcarriers respectively, which satisfy $\mathcal{S}_A \cup \mathcal{S}_N = \{-K/2, \ldots, K/2-1\}$. Let $s[k]$ denote the information symbol on the kth subcarrier. The transmitted passband signal is

$$\tilde{x}(t) = 2\text{Re}\left(\sum_{k\in\mathcal{S}_A} s[k] e^{j2\pi f_k t} g(t)\right), \qquad t \in [0, T'], \quad (4)$$

where $T' = (1+\beta)T + T_g$ is the ZP-OFDM block duration accounting for a zero guard time of length T_g; see Fig. 1 for an illustration. The Fourier transform of $\tilde{x}(t)$ for $f > 0$ is

$$\tilde{X}(f) = \sum_{k\in\mathcal{S}_A} s[k] G(f - f_k). \quad (5)$$

Assume that the channel consists of N_p discrete paths

$$h(\tau; t) = \sum_{p=1}^{N_p} A_p(t)\delta(\tau - \tau_p(t)), \quad (6)$$

where $A_p(t)$ and $\tau_p(t)$ are the amplitude and delay of the pth path. Within one OFDM block, we assume that (i) the amplitude does not change $A_p(t) \approx A_p$, and (ii) the path delay can be approximated as

$$\tau_p(t) \approx \tau_p - a_p t,$$

where τ_p is the initial delay and a_p is the Doppler rate of the pth path. As such, the received passband signal is

$$\tilde{y}(t) = \sum_{p=1}^{N_p} A_p \tilde{x}((1+a_p)t - \tau_p) + \tilde{n}(t), \quad (7)$$

where $\tilde{n}(t)$ is the additive noise.

As described in [1], [3], the receiver first performs a re-sampling operation on the received passband signal to remove the dominant Doppler effect, leading to $\tilde{z}(t) = \tilde{y}(t/(1+\hat{a}))$ where $(1+\hat{a})$ is the resampling factor. After downshifting, the baseband signal $z(t)$ is often sampled at the baseband rate $K\Delta f$, and hence the sampling interval is T/K. Since null subcarriers are placed at the edges of the signal band, this sampling rate does not incur any information loss. For each ZP-OFDM block, a total of

$$K' := (1+\beta)K + (T_g/T)K \quad (8)$$

time-domain samples are obtained, which contain all useful information about the current block.

The receivers in [1], [3] first compensate a mean Doppler shift (say ϵ Hz) on the baseband sequence, and then perform the FFT operation after overlap-adding. The FFT output on the kth subcarrier can be expressed as

$$\begin{aligned} z[k] &= Z(k/T + \epsilon) = \tilde{Z}(f_k + \epsilon) \\ &= \tilde{Y}((1+\hat{a})(f_k+\epsilon)), \quad k = -K/2, \ldots, K/2-1 \end{aligned} \quad (9)$$

where $Z(f)$, $\tilde{Z}(f)$, and $\tilde{Y}(f)$ are the Fourier transforms of $z(t)$, $\tilde{z}(t)$, and $\tilde{y}(t)$, respectively. Channel estimation and symbol detection in [1], [3] are performed based on the K frequency-domain samples $\{z[k]\}_{k=-K/2}^{K/2-1}$.

Obviously, the receivers in [1], [3] have not utilized all the information available for each ZP-OFDM block: only K frequently-domain samples are retained while there are $K' > K$ time-domain samples. In this paper, we investigate the benefit of frequency-domain oversampling in the context of underwater acoustic communication systems, and verify it using data collected from real experiments.

III. The Proposed Transceiver Design

We rely on the signal design in [5], where the data subcarriers are separated from the pilot subcarriers by at least two null subcarriers. This way, the inter-carrier interference (ICI) from direct neighbors can be explicitly considered at the receiver, so that good system performance can be achieved in underwater channels with large Doppler spread.

Specifically, subcarriers are divided into $K/8$ groups, with each group containing 8 subcarriers in the following pattern:

$$\begin{bmatrix} 0 & P & 0 & 0 & D & D & D & 0 \end{bmatrix}, \quad (10)$$

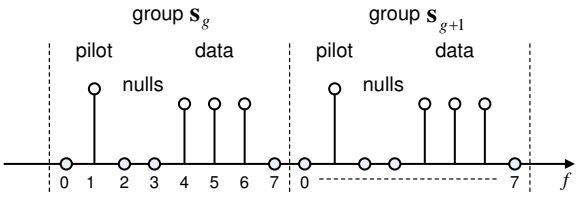

(a) Subcarrier index

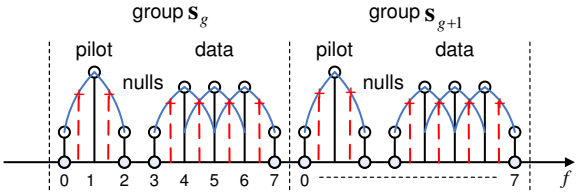

(b) solid lines are samples on the subcarriers, while dashed lines are samples in the middle of the subcarriers.

Fig. 2. The subcarrier index and illustration of oversampling with $\alpha = 2$.

where P and D denote a pilot symbol and a data symbol, respectively. The illustration is shown in Fig. 2. For the gth group, the index for the pilot subcarrier is $p_g = -K/2+8g+1$, and the indexes for the data subcarriers are $i_g - 1, i_g, i_g + 1$ where $i_g = -K/2 + 8g + 4$. Some subcarrier groups on the edge of the signal band are turned off.

A. Receiver Model

We next present the channel input-output relationship for the signal design in Fig. 2. Using frequency-domain oversampling with an oversampling factor α, an αK-point FFT operation is performed after padding $\{\alpha K - K'\}$ zeros to the baseband signal after Doppler shift compensation. Therefore, a total of αK frequency measurements are obtained. Define

$$\check{f}_{m'} = f_c + \frac{m'}{\alpha T}, \qquad m' = -\alpha K/2, \ldots, \alpha K/2 - 1. \quad (11)$$

The measurement $z[m']$ on the frequency $\check{f}_{m'}$ can be related to $z(t)$ as

$$z[m'] = \frac{1}{T}\int_0^{(1+\beta)T+T_g} z(t)e^{-j2\pi\epsilon t}e^{j2\pi\frac{m'}{\alpha T}t}dt. \quad (12)$$

Substituting (4) and (7) into (12) yields,

$$z[m'] = \sum_{p=1}^{N_p}\left[A'_p e^{-j2\pi(\check{f}_{m'}+\epsilon)\tau'_p}\left(\sum_{k\in\mathcal{S}_A}\varrho^{(p)}_{m',k}s[k]\right)\right] + v[m'], \quad (13)$$

where $v[m']$ is the additive noise and,

$$A'_p = \frac{A_p}{1+b_p}, \qquad \tau'_p = \frac{\tau_p}{1+b_p}, \qquad b_p = \frac{a_p - \hat{a}}{1+\hat{a}},$$
$$\varrho^{(p)}_{m',k} = G\left(\check{f}_{m'} - f_k + \frac{\epsilon - b_p\check{f}_{m'}}{1+b_p}\right).$$

We can rewrite (13) as

$$z[m'] = \sum_{k\in\mathcal{S}_A} H_{m',k}s[k] + v[m'], \quad (14)$$

where $k \in \{-K/2, \ldots, K/2-1\}$ is the subcarrier index, $m' \in \{-\alpha K/2, \ldots, \alpha K/2 - 1\}$ is the index for the FFT outputs, and

$$H_{m',k} = \sum_{p=1}^{N_p} A'_p e^{-j2\pi(\check{f}_{m'}+\epsilon)\tau'_p}\varrho^{(p)}_{m',k}. \quad (15)$$

B. Sparse Channel Estimation

Based on the assumption that the ICI beyond the direct subcarrier neighbors can be neglected, the receiver draws the following $2\alpha + 1$ frequency-domain samples for each pilot symbol transmitted:

$$z[m'] = H_{m',p_g}s[p_g] + v[m'], \quad (16)$$

where $m' = \alpha(p_g-1), \ldots, \alpha(p_g+1)$. The channel's frequency response estimate at frequency $\check{f}_{m'}$ is measured as $\hat{H}_{m',p_g} = z[m']/s[p_g]$. Corresponding to $K/8$ pilot subcarriers, a total of $(2\alpha+1)K/8$ channel measurements can be collected.

Using compressive sensing techniques, the receiver explores the sparse nature of the underwater acoustic channel and jointly estimate the complex gain, the Doppler scale, and the delay $\{A'_p, b_p, \tau'_p\}$ corresponding to N_p discrete paths; see [3] for more details. The channel coefficients needed for data detection are then reconstructed using (15).

C. MMSE Channel Equalization

Channel equalization is applied on each group separately. For the gth group with three data symbols $s[i_g-1], s[i_g], s[i_g+1]$, the related channel outputs are:

$$\underbrace{\begin{pmatrix} z[\alpha(i_g-2)] \\ \vdots \\ z[\alpha i_g] \\ \vdots \\ z[\alpha(i_g+2)] \end{pmatrix}}_{:=\mathbf{z}_g} = \underbrace{\begin{pmatrix} v[\alpha(i_g-2)] \\ \vdots \\ v[\alpha i_g] \\ \vdots \\ v[\alpha(i_g+2)] \end{pmatrix}}_{:=\mathbf{v}_g} + \quad (17)$$
$$\underbrace{\begin{pmatrix} H_{\alpha(i_g-2),(i_g-1)} & 0 & 0 \\ \vdots & \vdots & \vdots \\ H_{\alpha i_g,(i_g-1)} & H_{\alpha i_g,i_g} & H_{\alpha i_g,(i_g+1)} \\ \vdots & \vdots & \vdots \\ 0 & 0 & H_{\alpha(i_g+2),(i_g+1)} \end{pmatrix}}_{:=\mathbf{H}_g} \underbrace{\begin{pmatrix} s[i_g-1] \\ s[i_g] \\ s[i_g+1] \end{pmatrix}}_{:=\mathbf{d}_g}$$

The vector $\mathbf{z}_g$ is of length $4\alpha + 1$. With $\alpha = 1$ in the conventional receiver, 5 measurements are used to decode 3 symbols, while an oversampling factor of $\alpha = 2$ leads to 9 available measurements to decode 3 symbols.

The output of the MMSE equalizer is

$$\hat{\mathbf{d}}_g = \left(\mathbf{H}_g^H\mathbf{H}_g + \frac{N_0}{E_s}\mathbf{I}_3\right)^{-1}\mathbf{H}_g^H\mathbf{z}_g, \quad (18)$$

where E_s is the symbol energy and N_0 is the noise covariance in the frequency-domain. Note that in (18), we have approximated the noise to be white. The noise color can be incorporated in our future work. Alternatively, one can pad $\alpha K - K'$ noise samples rather than zeros for the αK-point FFT operation, so that the noise is white.

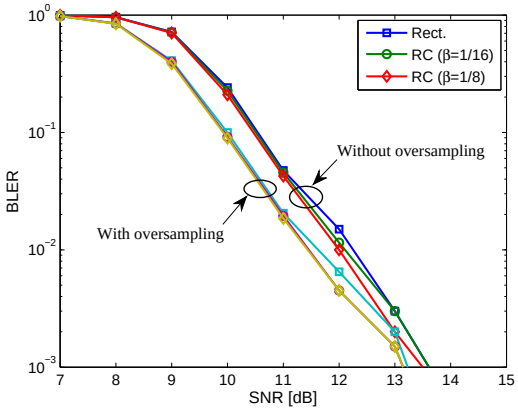

Fig. 3. Simulated BLER performance, $\sigma_v = 0.10$ m/s

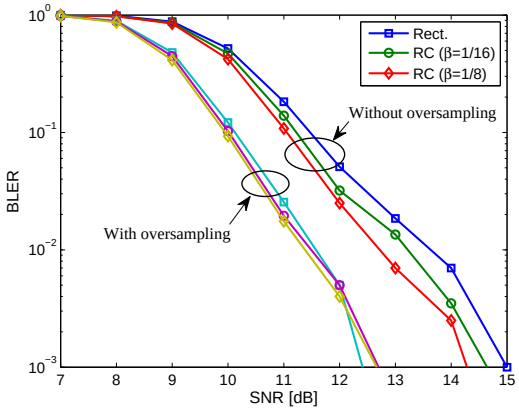

Fig. 4. Simulated BLER performance, $\sigma_v = 0.25$ m/s

IV. Numerical Simulation

The sparse channel consists of 10 discrete paths, where the inter-arrival time follows an exponential distribution with a mean of 0.5 ms. The amplitudes are Rayleigh distributed with the average power decreasing exponentially with the delay, where the difference between the beginning and the end of the guard time of 13.1 ms is 20 dB. The Doppler rate of each path is drawn from a zero mean Gaussian distribution with the standard deviation of $\sigma_v f_c/c$, where σ_v denotes the standard deviation of the platform velocity, and c is the sound speed in water being set to 1500 m/s. Hence, the maximum possible Doppler is about $\sqrt{3}\sigma_v f_c/c$.

The ZP-OFDM signal parameters are tailored according to the setting of the SPACE08 experiment in Table I, with the only exception of $T_g = 13.1$ ms. The subcarrier allocation in Fig. 2 is adopted. Out of the $M = K/8 = 128$ groups, 8 groups on each edge of the signal band are turned off for the band protection, while the pilot subcarriers therein are still used to carry pilot symbols. Hence, there are $|\mathcal{S}_P| = 128$ pilot subcarriers and $|\mathcal{S}_D| = 384$ data subcarriers in total. The data symbols are encoded with a rate-$1/2$ nonbinary LDPC code [9] and modulated with a 16-QAM constellation, which leads to a data rate R as:

$$R = \frac{1}{2}\frac{|\mathcal{S}_D| \cdot \log_2 16}{(1+\beta)T + T_g}. \tag{19}$$

For raised-cosine windows with $\beta = 0,\ 1/16,\ 1/8$, the overall data rates are $R = 6.5,\ 6.2,\ 5.9$ kb/s, respectively.

Fig. 3 and Fig. 4 depict the block-error-rate (BLER) performance of the receivers with or without frequency-domain oversampling using different windows, with $\sigma_v = 0.10$ m/s and $\sigma_v = 0.25$ m/s, respectively. A total of 2000 Monte Carlo runs are used. With the conventional sampling method, the BLER performance of the raised-cosine window is better than that of the rectangular window, and the performance gap improves as the roll-off factor increases. However, with frequency-domain oversampling, the performance gap between the two types of windows becomes very small. Compared with the windowing operation, the performance gain of the frequency-domain oversampling receiver is more pronounced, especially in the scenario with large velocity deviation.

V. SPACE08 Experimental Results

This experiment was held off the coast of Martha's Vineyard, Massachusetts, from Oct. 14 to Nov. 1, 2008. The water depth was about 15 meters. Among all the six receivers, we only consider the data collected by three receivers, labeled as S1, S3, S5, which were 60 m, 200 m, and 1000 m away from the transmitter. Each receiver array consists of twelve hydrophones. During the experiment, two storm cycles showed up, one around Julian date 297 and the other around Julian date 300. The latter storm was more severe. We only consider the data recorded from Julian dates 299-301, the days around the second storm cycle. For each day, there are ten recorded files, each consisting of twenty OFDM blocks. Parameter settings of this experiment are summarized in Table I.

TABLE I
OFDM Parameters in Simulation and SPACE08 Experiment.

f_c	13 kHz
B	9.77 kHz
K	1024
T	104.86 ms
$\Delta f := 1/T$	9.54 Hz
T_g	24.6 ms

A. BLER performance with stationary receivers

Due to the mild Doppler effect, the resampling operation is not performed. With a 16-QAM constellation and a rate-1/2 nonbinary LDPC code, the BLER performance averaged over Julian dates 299-301 by combining an increasing number of phones is shown in Fig. 5. Compared with the conventional sampling, frequency-domain oversampling helps to achieve similar performance with less number of phones. Obviously, more frequency-domain observations leads to better channel estimation and symbol detection performance.

B. BLER performance with moving receivers

With the same transmitter, additional data were recorded by an 8-element array, towed by a vehicle moving at the speed of about 1 m/s. Four runs of data were collected, each with twenty OFDM blocks. The estimated resampling factor for

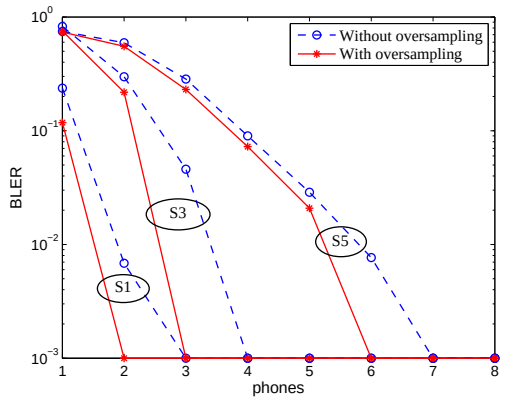

Fig. 5. BLER performance with stationary receivers; SPACE08.

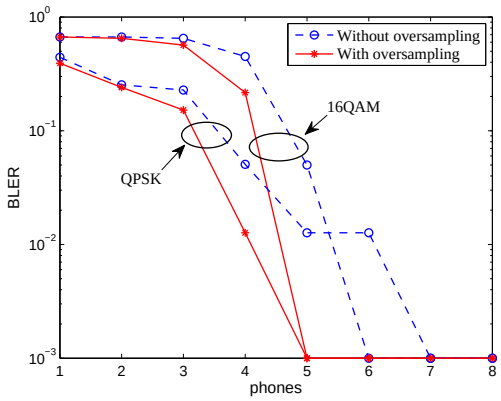

Fig. 6. BLER performance with moving receivers; SPACE08.

each run is $[1.0006,\ 0.9991,\ 0.99913,\ 1.0001]$, corresponding to a moving speed $[0.85,\ 1.3,\ 1.35,\ 0.15]$ m/s, respectively. The BLER performance of the conventional sampling method and the frequency oversampling method are shown in Fig. 6, where the resmapling operation was not applied for the data pre-processing as we would like to compare these two methods in a scenario with large Doppler spreads. In such a scenario, the performance improvement due to frequency oversampling is more significant.

VI. WHOI09 Experimental Results

This experiment was carried out in the Buzzards Bay, Massachusetts, from Dec. 07 to Dec. 08, 2009. The water depth was about 15 meters. Two buoy-based receivers were deployed at 1000 m and 2000 m away from the transmitter, each with 4 hydrophones. There were three transmissions in total, each consisting of 15 OFDM blocks using the rectangular window, 15 blocks using a raised-cosine window with $\beta = 1/16$, and the other 15 blocks using a raised-cosine window with $\beta = 1/8$. The ZP-OFDM parameters are: $f_c = 31$ kHz, $B = 10$ kHz, $K = 1024$, $T = 102.4$ ms, and $T_g = 24$ ms.

Due to the calm environment and large input SNR, most received blocks can be decoded with just one phone, hence, the performance difference between different settings is hard to tell. To enlarge the difference, the received signal is decoded without the Doppler shift compensation step [1]. We here only consider the signal received at the buoy 2000 meters away from the transmitter. The number of decoded blocks in error out of the total 45 blocks are shown in Table II, with 16 QAM constellation and rate-1/2 nonbinary LDPC coding [9]. The benefit of frequency-domain oversampling is evident.

TABLE II

The number of decoded blocks in error out of 45 blocks; Without Doppler shift compensation

	# of Phones	Rect.	RC (1/16)	RC (1/8)
Without oversampling	1	10	11	6
	2	1	0	1
	3	0	0	0
With oversampling	1	0	0	0
	2	0	0	0
	3	0	0	0

VII. Conclusion

In this paper, we presented a zero-padded OFDM transceiver design with rectangular and raised-cosine pulse-shaping windows for underwater acoustic communications. Numerical and experimental results demonstrated that frequency-domain oversampling improves the system performance considerably, and the gain becomes larger as the channel Doppler spread increases. A raised-cosine pulse-shaping window can improve the performance relative to a rectangular window, however, the performance gain is much less than that brought by frequency-domain oversampling in the considered OFDM system dealing with underwater channels with large Doppler spread.

Acknowledgement

We thank Dr. J. Preisig for the SPACE08 experiment, and Mr. L. Freitag for the WHOI09 experiment.

References

[1] B. Li, S. Zhou, M. Stojanovic, L. Freitag, and P. Willett, "Multicarrier communication over underwater acoustic channels with nonuniform Doppler shifts," *IEEE J. Ocean. Eng.*, vol. 33, no. 2, Apr. 2008.

[2] M. Stojanovic, "Low complexity OFDM detector for underwater channels," in *Proc. of OCEANS Conf.*, Boston, MA, Sept. 18-21, 2006.

[3] C. R. Berger, S. Zhou, J. Preisig, and P. Willett, "Sparse channel estimation for multicarrier underwater acoustic communication: From subspace methods to compressed sensing," *IEEE Trans. Signal Processing*, pp. 1708–1721, Mar. 2010.

[4] B. Muquet, Z. Wang, G. B. Giannakis, M. de Courville, and P. Duhamel, "Cyclic-prefixing or zero-padding for wireless multicarrier transmissions?" *IEEE Trans. Commun.*, pp. 2136–2148, Dec. 2002.

[5] S. Mason, C. R. Berger, S. Zhou, K. Ball, L. Freitag, and P. Willett, "An OFDM design for underwater acoustic channels with Doppler spread," in *Proc. of the 2009 DSP & SPE Workshop*, Marco Island, FL, Jan. 2009.

[6] J. G. Proakis, *Digital Communications*, 4th ed. McGraw-Hill, 2001.

[7] M. Luise, M. Marselli, and R. Reggiannini, "Low-complexity blind carrier frequency recovery for OFDM signals over frequency-selective radio channels," *IEEE Trans. Commun.*, vol. 50, no. 7, pp. 1182–1188, 2002.

[8] Q. Shi and Y. Karasawa, "Frequency-domain oversampling for OFDM systems: exploiting inter-carrier interference and multipath diversity," in *Proc. of IEEE Intl. Symp. on Communications and Information Technology*, 2009, pp. 1097–1101.

[9] J. Huang, S. Zhou, and P. Willett, "Nonbinary LDPC coding for multicarrier underwater acoustic communication," *IEEE J. Select. Areas Commun.*, vol. 26, no. 9, pp. 1684–1696, Dec. 2008.